# Talbot effect interpreted by number theory

**María Teresa Flores-Arias, María Victoria Pérez, Carlos Gómez-Reino, and Carmen Bao**

*Laboratorio de Optica, Departamento de Física Aplicada, Facultad de Física, Universidade de Santiago de Compostela, Campus Sur, E15782, Santiago de Compostela, Galicia, Spain*

**Carlos R. Fernández-Pousa**

*Departamento de Ciencia y Tecnología de Materiales, División de Optica, Edificio la Galia, Universitat Miguel Hernandez, E03202 Elx, Alacant, Spain*

Received February 20, 2001; revised manuscript received April 26, 2001; accepted April 30, 2001

An interpretation of the Talbot effect in a tapered gradient-index medium by number theory as the output/input relationship between the integer and the noninteger difference of position and the slope of rays is presented. Unit cell and transverse magnification for Talbot images are evaluated, and two criteria for angular magnification are defined. The study is particularized to a finite set of diffracted rays. 

*OCIS codes:* 070.6760, 110.0110.

## 1. INTRODUCTION

The integer and fractional Talbot effects in a homogeneous medium are well known in optics and have received wide attention.[1,2] Recently authors have described the integer and fractional Talbot effects in a tapered gradient-index (GRIN) medium.[3,4]

The Talbot effect has been interpreted as self-images of a periodic object by Fourier optics, as multiple-slit diffraction patterns in the Fresnel and Fraunhofer domains, and as a superposition of a proper set of nondiffracting beams, or modes, in either free space or inhomogeneous media.[1,2,5–8] The purpose of this paper is to explain the Talbot effect from the viewpoint of number theory as the output/input relationship between the integer and the noninteger difference of position and the slope of rays coming from a periodic object that intersect in equispaced points at given planes. We obtain by geometrical methods the axial positions of Talbot images, both integer and fractional, and the structure of rays in the unit cells of those images. For clarity and simplicity the discussion is restricted to one-dimensional periodic objects. An infinite number of rays coming from the object are considered. Finally, we apply the study to a finite number of rays in order to evaluate the number of Talbot images that can be visualized by simple ray-tracing techniques.

## 2. STATEMENT OF THE PROBLEM

Let us consider a tapered GRIN medium characterized by a transverse parabolic refractive index modulated by an axial index and whose refractive index is given by

$$n^2(x, z) = n_0^2[1 - g^2(z)x^2], \tag{1}$$

where $n_0$ is the index at the $z$ optical axis and $g(z)$ is the taper function that describes the evolution of the transverse index along the $z$ axis.

We assume that a one-dimensional periodic object with period $p$, of infinite dimensions, is located at the input of this medium and is illuminated by a linear source of wavelength $\lambda$ located at a distance $d$ from the input. The periodic object consisting of a Dirac comb is represented by

$$T(x_0) = \sum_{h=-\infty}^{+\infty} \delta(x_0 - hp) = \frac{1}{p} \sum_{h=-\infty}^{+\infty} \exp\left(-i\frac{2\pi h x_0}{p}\right), \tag{2}$$

where $\delta$ is the Dirac delta function.

We apply the ray-matrix method (*ABCD* law) to the study of light propagation through the hybrid optical structure shown in Fig. 1. On the input face, light undergoes refraction and diffraction, and at a point $x_{0h} = hp$, where $h$ is an integer, the slope of the rays is given by

$$\dot{x}_{0h} = \dot{x}_{0h}^r + \dot{x}_{0h}^m, \tag{3}$$

where $\dot{x}_{0h}^r$ and $\dot{x}_{0h}^m$ are the slopes of the refracted and the $m$th order diffracted rays, respectively, and the dot denotes the derivative with respect to $z$.

$\dot{x}_{0h}^r$ and $\dot{x}_{0h}^m$ can be expressed in terms of the distance to the source and the period of the object, under paraxial approximation, as

$$\dot{x}_{0h}^r = \frac{x_{0h}}{n_0 d}, \tag{4}$$

$$\dot{x}_{0h}^m = \frac{m\lambda}{n_0 p}. \tag{5}$$

The ray position and the ray slope at any $z > 0$ are related to the ray position and the ray slope at the input face by the *ABCD* law,[9]

$$\begin{pmatrix} x(z) \\ \dot{x}(z) \end{pmatrix} = \begin{bmatrix} H_2(z) & H_1(z) \\ \dot{H}_2(z) & \dot{H}_1(z) \end{bmatrix} \begin{pmatrix} x_{0h} \\ \dot{x}_{0h} \end{pmatrix}, \tag{6}$$

 

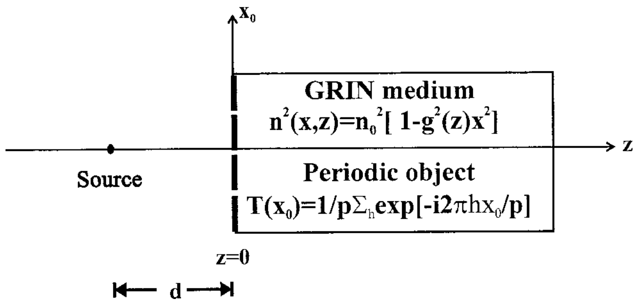


Fig. 1. Geometry for evaluating the complex amplitude distribution in a tapered GRIN medium due to a periodic object located at $z = 0$ and illuminated by a cylindrical uniform beam.

where $H_1$, $H_2$ and $\dot{H}_1$, $\dot{H}_2$ are the position and the slope, respectively, of the axial and the field rays at $z$; that is,

$$H_1(z) = [g_0 g(z)]^{-1/2} \sin\left[\int_0^z g(z')\mathrm{d}z'\right] = -[g_0 g(z)]^{-1}\dot{H}_2(z), \tag{7}$$

$$H_2(z) = \left[\frac{g_0}{g(z)}\right]^{1/2} \cos\left[\int_0^z g(z')\mathrm{d}z'\right] = \frac{g_0}{g(z)}\dot{H}_1(z), \tag{8}$$

$g_0$ being the value of $g$ at $z = 0$. Initial conditions for both rays are given by

$$H_1(0) = 0, \tag{9a}$$

$$\dot{H}_1(0) = 1 \tag{9b}$$

$$H_2(0) = 1, \tag{10a}$$

$$\dot{H}_2(0) = 0, \tag{10b}$$

such that

$$\dot{H}_1(z)H_2(z) - H_1(z)\dot{H}_2(z) = 1. \tag{11}$$

When Eqs. (3) and (4) have been taken into account, Eq. (6) can be rewritten as

$$\begin{pmatrix} x(z) \\ \dot{x}(z) \end{pmatrix} = \begin{bmatrix} H_2(z) + \dfrac{H_1(z)}{n_0 d} & H_1(z) \\ \dot{H}_2(z) + \dfrac{\dot{H}_1(z)}{n_0 d} & \dot{H}_1(z) \end{bmatrix} \begin{pmatrix} x_{0h} \\ \dot{x}_{0h}^m \end{pmatrix} \tag{12}$$

where the refraction has been included in the ray-transfer matrix. By simplicity, we will denote the position and slope of the diffracted ray at the input, $x_{0h}$ and $\dot{x}_{0h}^m$, by the integers $h$ and $m$, respectively. Integer $h$ denotes the unit-cell number of the periodic object, called cell number henceforth, and integer $m$ indicates diffraction order.

Equation (12) is the key to the problem; it will enable us to obtain the most important conditions in first-order optics. It can be written, in compact form, as

$$\overset{(\cdot)}{x}(z) = p\overset{(\cdot)}{A}(z)[h + m\overset{(\cdot)}{\xi}(z)], \tag{13}$$

where

$$\overset{(\cdot)}{\xi}(z) = \frac{\overset{(\cdot)}{B}(z)}{p\overset{(\cdot)}{A}(z)}, \tag{14}$$

$$\overset{(\cdot)}{A}(z) = \overset{(\cdot)}{H}_2(z) + \frac{\overset{(\cdot)}{H}_1(z)}{n_0 d}, \tag{15}$$

$$\overset{(\cdot)}{B}(z) = \frac{\lambda\overset{(\cdot)}{H}_1(z)}{n_0 p}. \tag{16}$$

From Eq. (13) it follows that the position and slope of any ray at $z$ depend on cell number and diffraction order at the input.

## 3. TALBOT, IMAGE, AND FOURIER TRANSFORM CONDITIONS

In this section we will study the ray positions given by Eq. (13) at $z > 0$. We want to find the axial lengths $z = \bar{z}$ where the rays coming from the input intersect at equispaced points independently of their cell number and diffraction order at the input.

Let $z = \bar{z}$ be a position in the GRIN medium; then there exists a periodic distribution of points where rays intersect at $\bar{z}$ if $x(\bar{z}) = h'p'(\bar{z})$ holds, where $p'(\bar{z}) > 0$ is the period and $h' \in Z$ is the cell number at $\bar{z}$.

At the positions where rays intersect at $\bar{z}$ we have that

$$h + m\xi(\bar{z}) = \frac{h'p'(\bar{z})}{pA(\bar{z})}, \tag{17}$$

where Eq. (13) has been used.

The equispacing condition, Eq. (17), can be transformed into a purely algebraic condition that concerns only the $\xi(z)$ function. As we will show, Eq. (17) is equivalent to the fact that $\xi(z)$ is a rational number,

$$\xi(\bar{z}) = \beta/\alpha, \tag{18}$$

for positive integers $\alpha$ and $\beta$. Indeed, if we consider two rays specified by $(h_1, m_1)$ and $(h_2, m_2)$, they will intersect a given plane $z = \bar{z}$ at the positions

$$h_1'p'(\bar{z}) = pA(\bar{z})[h_1 + m_1\xi(\bar{z})], \tag{19a}$$

$$h_2'p'(\bar{z}) = pA(\bar{z})[h_2 + m_2\xi(\bar{z})], \tag{19b}$$

therefore $\xi(z)$ has to be of the form

$$\xi(\bar{z}) = \frac{h_1'h_2 - h_2'h_1}{m_1h_2' - m_2h_1'}, \tag{20}$$

and thus $\xi(z)$ is necessarily a rational number. This condition is also sufficient, since if we assume Eq. (18), the form of the positions at plane $z = \bar{z}$ is

$$x(\bar{z}) = \frac{pA(\bar{z})}{\alpha}(h\alpha + m\beta), \tag{21}$$

which are integer multiples of the quantity $pA(\bar{z})/\alpha$, and thus positions give rise to an equispaced pattern.

Condition (18) determines the planes $z = \bar{z}$ where rays are focused at equispaced points. $\beta/\alpha$ is any fractional number, and thus it can be decomposed as

$$\beta/\alpha = \nu + \beta'/\alpha', \tag{22}$$

with $\nu$ an integer number and $\beta'/\alpha'$ a fractional number lower than 1, $\alpha'$, $\beta'$ being co-prime integers. This decomposition can be used to define planes, depending on the value of the fraction $\beta/\alpha$. If $\beta/\alpha = \nu$, the planes $\bar{z} = z_\nu$ determined by the condition

$$\xi(z_\nu) = \nu \tag{23}$$

are the integer Talbot planes, and the planes $\bar{z} = z_{\beta'/\alpha'}$ that verify

$$\xi(z_{\beta'/\alpha'}) = \beta'/\alpha' \tag{24}$$

are the fractional Talbot planes lying before the first ($\nu = 1$) integer Talbot planes. In general, solutions of condition (18) are fractional Talbot planes lying between two consecutive integer Talbot planes.

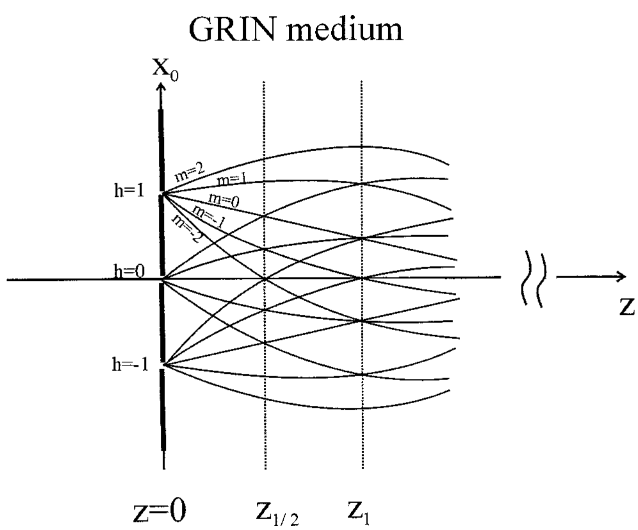


Fig. 2. Integer and fractional Talbot images for $\beta'/\alpha' = 1/2$ and $\nu = 1$.

We now analyze Eqs. (23) and (24) in order to find physical meaning. We consider two rays, $(h_1, m_1)$ and $(h_2, m_2)$. When the two rays intersect at $\bar{z} = z_\nu$, we have

$$\nu = \frac{h_1 - h_2}{m_2 - m_1}, \tag{25}$$

where Eqs. (17) and (23) have been used. From Eq. (25) it follows that at $z_\nu$ the difference between the cell numbers at the input must be an integer multiple of the difference between diffraction orders at the input (Fig. 2).

Similarly, if two rays intersect at $z_{\beta'/\alpha'}$ we can write

$$\frac{\beta'}{\alpha'} = \frac{h_1 - h_2}{m_2 - m_1}, \tag{26}$$

and now the difference between cell numbers at the input is not an integer multiple of the difference between diffraction orders (Fig. 2).

Conditions (25) and (26) for obtaining a periodic distribution of points are called integer and fractional Talbot conditions, respectively.[3,4]

On the other hand, of particular importance are two cases when $\xi(\bar{z})$ cancels or tends to infinity; that is,

$$\xi(z_{\text{im}}) = 0 \qquad \text{if } \beta = 0 \text{ or } B(z_{\text{im}}) = 0, \tag{27}$$

$$\xi(z_{\text{ft}}) = \infty \qquad \text{if } \alpha = 0 \text{ or } A(z_{\text{ft}}) = 0, \tag{28}$$

where Eqs. (14) and (18) have been used.

Equation (27) indicates that all the rays coming from the same input cell ($h_1 = h_2$) with different diffraction orders ($m_1 \neq m_2$) intersect at planes $\bar{z} = z_{\text{im}}$ such that $B(z_{\text{im}}) = 0$, and, in the same way, from Eq. (28) it follows that rays coming from different cells ($h_1 \neq h_2$) with the same diffraction order ($m_1 = m_2$) intersect at planes $\bar{z} = z_{\text{ft}}$ such that $A(z_{\text{ft}}) = 0$. Equations (27) and (28) are the well-known image and Fourier transform conditions in GRIN media, respectively (Fig. 3). The two conditions can be expressed respectively as[9]

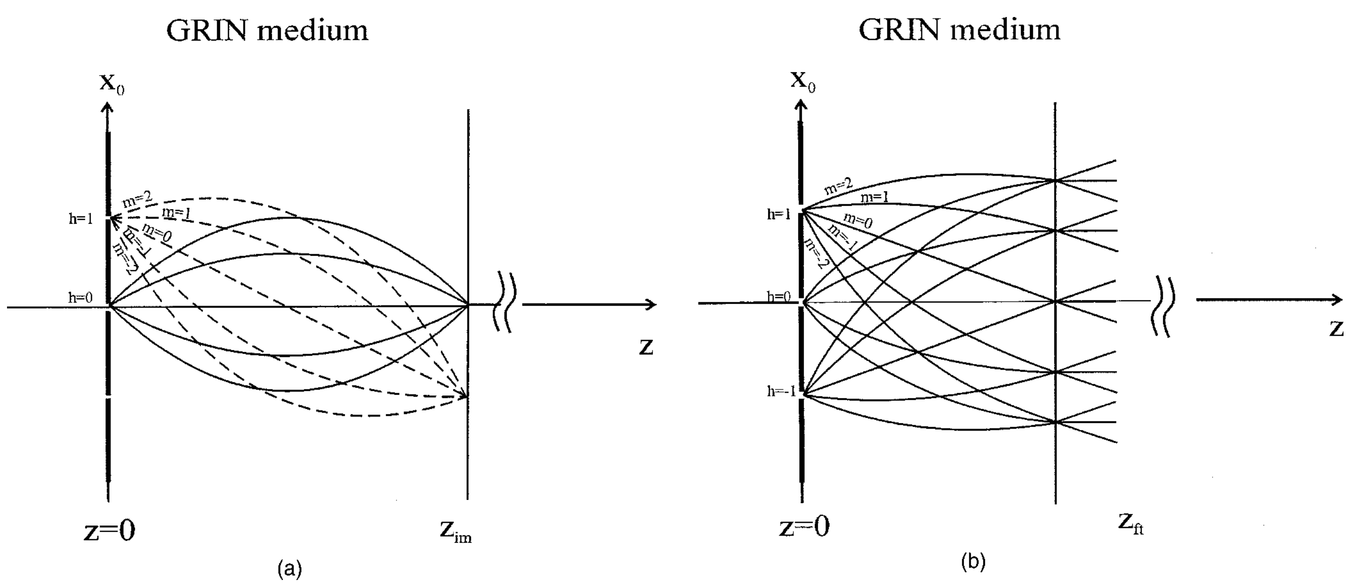


Fig. 3. Ray tracing for (a) image and (b) Fourier transform conditions.

$$H_1(z_{\mathrm{im}}) = 0, \tag{29}$$

$$H_2(z_{\mathrm{ft}}) = -\frac{H_1(z_{\mathrm{ft}})}{n_0 d}, \tag{30}$$

where Eqs. (15) and (16) have been used.

## 4. TALBOT IMAGES: UNIT CELL AND TRANSVERSE MAGNIFICATION

It is well known that Talbot condition (18) provides images that are not quite like the conventional ones given by Eq. (29). Each integer or fractional Talbot image arises from intersections between rays from all unit cells in the grating. We will show that these fractional Talbot images of the original grating are formed by unit cells of period $pA(z_{\beta'/\alpha'})$ consisting of $\alpha'$ points equally spaced by the interval[4] $pA(z_{\beta'/\alpha'})/\alpha'$. Each of these points inside the same unit cell will be specified by the intracell number. For that, it will be necessary to prove, on the one hand, that the diffraction orders of the rays passing through each point of unit cell are different and, on the other hand, that the diffraction orders of the rays crossing homologous points at any two unit cells are equal.

This proof will be treated from the viewpoint of number theory; therefore let us rewrite Eq. (13) at fractional Talbot positions as

$$x(z_{\beta'/\alpha'}) = \frac{pA(z_{\beta'/\alpha'})}{\alpha'}(h\alpha' + m\beta') = p'(z_{\beta'/\alpha'})u, \tag{31}$$

where $u$ is an integer number representing the intracell number, that is, it specifies the position of rays inside a unit cell. Thus, the intracell number at the fractional Talbot position is expressed in terms of cell number and diffraction order at the input as

$$u = h\alpha' + m\beta', \tag{32}$$

and the separation between consecutive intracell numbers, is expressed as

$$p'(z_{\beta'/\alpha'}) = \frac{pA(z_{\beta'/\alpha'})}{\alpha'}. \tag{33}$$

If we denote by $(\bar{h}, \bar{m})$ a particular solution of Eq. (32) for $u = 1$ (see Refs. 10 and 11),

$$\bar{h}\alpha' + \bar{m}\beta' = 1, \tag{34}$$

then the general solution for Eq. (32) is given by (see Appendix A)

$$\tilde{h} = u\bar{h} - \beta' t, \tag{35a}$$

$$\tilde{m} = u\bar{m} + \alpha' t, \tag{35b}$$

for any integer $t$.

With this general solution we can now probe whether the diffraction orders of the rays passing through each point in unit cell are different. Let $u = i$ and $u = j$, $i \neq j$, be two intracell numbers specifying points of the unit cell such that $i, j = 1, 2, \ldots \alpha'$ with $\alpha' > 1$. Notice that this choice implies

$$1 \leqslant |i - j| \leqslant \alpha' - 1. \tag{36}$$

According to Eq. (35b), the diffraction orders passing through $i$ and $j$ are given by $i\bar{m} + \alpha' t$ and $j\bar{m} + \alpha'\tilde{t}$, for integers $t$ and $\tilde{t}$, respectively. If we assume that the two rays are the same order, then

$$i\bar{m} + \alpha' t = j\bar{m} + \alpha'\tilde{t}; \tag{37}$$

that is,

$$\bar{m} = \frac{\alpha'(t - \tilde{t})}{j - i}. \tag{38}$$

Since $\bar{m}$ is an integer, $j - i$ must divide either into $\alpha'$, into $t - \tilde{t}$, or both. Thus, in the most general case, we can parameterize $j - i$ as

$$j - i = a_1 a_2, \tag{39}$$

with integer $a_1$ dividing $\alpha'$ and integer $a_2$ dividing $t - \tilde{t}$, so that

$$\bar{m} = r_1 r_2, \tag{40}$$

with $r_1, r_2$ integer numbers such that

$$r_1 = \frac{\alpha'}{a_1}, \tag{41a}$$

$$r_2 = \frac{t - \tilde{t}}{a_2}. \tag{41b}$$

Substitution of Eq. (40) into Eq. (34) gives

$$r_1(\bar{h}a_1 + \beta' r_2) = 1, \tag{42}$$

where Eq. (41a) has been used. Since the two factors on the left-hand side of Eq. (42) are integers, we must have

$$|r_1| = 1, \tag{43a}$$

$$|\bar{h}a_1 + \beta' r_2| = 1 \tag{43b}$$

so that from Eqs. (43a) and (41a) we get

$$|a_1| = \alpha' > 1, \tag{44}$$

and therefore

$$|j - i| = |a_1||a_2| \geqslant |a_1| = \alpha', \tag{45}$$

which contradicts Eq. (36). This contradiction is also achieved if we assume in Eq. (39) that $j - i$ divides only into $\alpha'$. Then the only remaining possibility is that $j - i$ divides only into $t - \tilde{t}$. Thus let us assume that

$$\frac{t - \tilde{t}}{j - i} = r, \qquad \forall\, r \in Z \tag{46}$$

for some integer number $r$.

Substituting Eq. (46) into Eq. (38) we get

$$\bar{m} = \alpha' r, \tag{47}$$

and inserting Eq. (47) into Eq. (34) yields

$$\alpha'(\bar{h} + r\beta') = 1, \tag{48}$$

whose solution is given by

$$|\alpha'| = 1, \tag{49}$$

which is incompatible with Eq. (36), since $\alpha'$, $\beta'$ are coprime integers. In short, it has been proved that the diffraction orders of the rays passing through point $j$ are different from those passing through $i$. The set of points with this property define unit cell.

The second part of the proof shows that the rays passing at $z_{\beta'/\alpha'}$ through positions $u$ and $u + \alpha'$ corresponding to two consecutive unit cells have equal diffraction orders and come from consecutive positions in the input plane. Then if a ray crossing $u$ has diffraction order equal to that of a ray crossing $u + \alpha'$, from Eq. (35b) we have

$$u\bar{m} + \alpha' t = (u + \alpha')\bar{m} + \alpha'\tilde{t}, \tag{50}$$

which yields

$$t = \tilde{t} + \bar{m}. \tag{51}$$

Equation (51) represents the condition for which two rays passing through $u$ and $u + \alpha'$ at $\bar{z} = z_{\beta'/\alpha'}$ have equal diffraction order.

Similarly, these two rays come from positions at the input given by

$$x_{0h} = ph = p(u\bar{h} - \beta' t), \tag{52a}$$

$$x_{0\tilde{h}} = p\tilde{h} = p[(u + \alpha')\bar{h} - \beta'\tilde{t}], \tag{52b}$$

where Eq. (35a) has been used.

From Eqs. (52) it follows that the position difference at the input between the two rays, taking into account condition (51), is expressed as

$$\Delta x_0 = x_{0\tilde{h}} - x_{0h} = p(\bar{h}\alpha' + \bar{m}\beta') = p, \tag{53}$$

where Eq. (34) has been used.

Then the two rays with the same diffraction order at $z_{\beta'/\alpha'}$ come from two consecutive unit cells of the periodic object at the input.

Thus the unit cell of the fractional Talbot image is formed by $\alpha'$ points equally spaced by an intracell period given by

$$p' = \frac{pA(z_{\beta'/\alpha'})}{\alpha'}(u + 1) - \frac{pA(z_{\beta'/\alpha'})}{\alpha'}u = \frac{pA(z_{\beta'/\alpha'})}{\alpha'}. \tag{54}$$

Likewise, $\alpha' p' = pA(z_{\beta'/\alpha'})$ is the period of the fractional Talbot image and $A(z_{\beta'/\alpha'})$ becomes the transverse magnification. These facts capture the physics of Talbot effect in which $\alpha'$ images of the object unit cell are reproduced in each unit cell of the Talbot image, with intracell spacing given by Eq. (54) and transverse magnification $A$.

For the integer Talbot image a periodic distribution of ray positions is obtained, and these ray positions are given by

$$x(z_\nu) = pA(z_\nu)[h + \nu m] = p' h'(z_\nu), \tag{55}$$

where Eqs. (13) and (23) have been used.

Equation (54) provides the period of the integer image, which can be expressed as

$$p' = pA(z_\nu), \tag{56}$$

$A(z_\nu)$ being the transverse magnification. Note that in the case of the integer Talbot image, the unit cell contains only one point.

We study transverse magnification for a particular tapered GRIN medium with a divergent linear taper function given by

$$g(z) = \frac{g_0}{1 + (z/L)}, \tag{57}$$

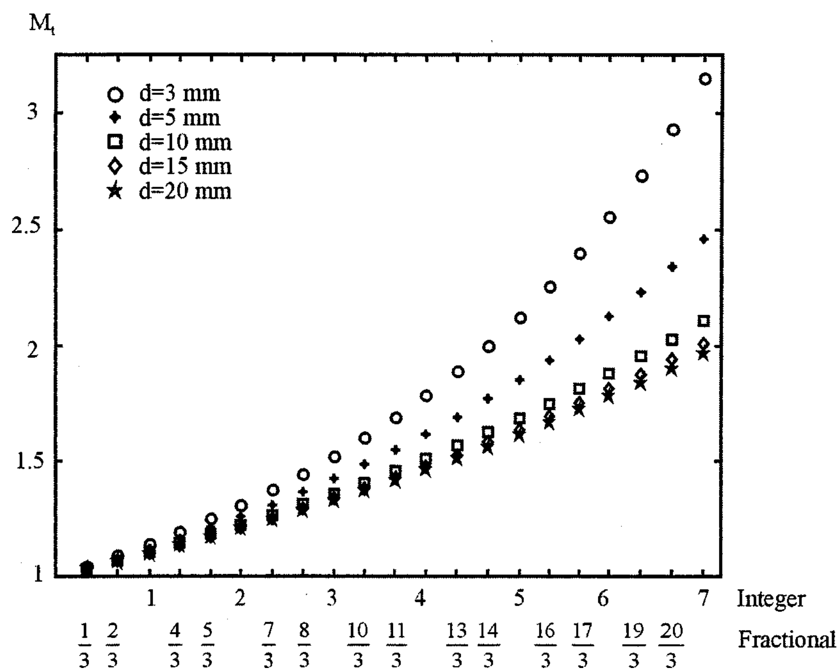


Fig. 4. Transverse magnification of Talbot images versus self-image number for different values of $d$. Calculations have been made for $n_0 = 1.5$, $g_0 = 0.01\ \mathrm{mm}^{-1}$, $\lambda = 0.7\ \mu\mathrm{m}$, $L = 1$ mm, and $p = 9\ \mu\mathrm{m}$.

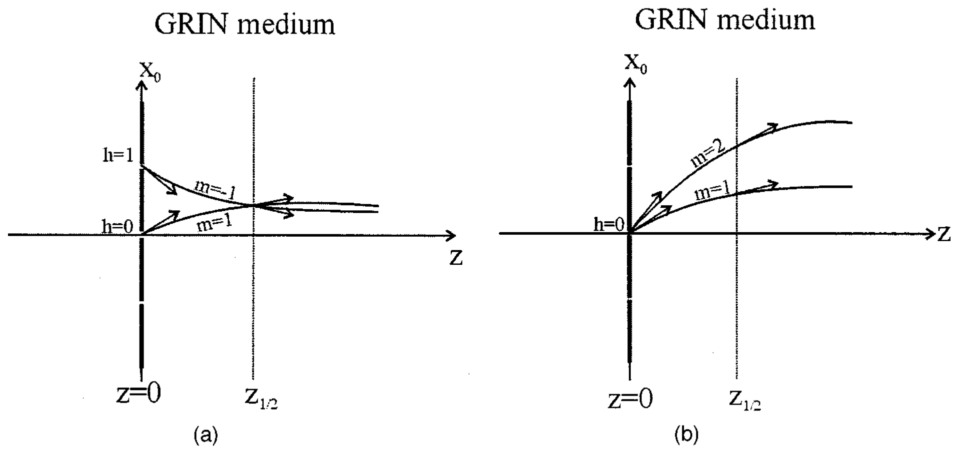


Fig. 5. Ray tracing for (a) the first and (b) the second criterion of angular magnification.

$L$ being the distance from $z = 0$ to the common apex of the equi-index lines.

Figure 4 represents transverse magnification versus the self-image number for different values of the curvature radius of the incident beam. On the one hand, for a given $d$, transverse magnification increases with self-image number. On the other hand, for a given Talbot position, transverse magnification decreases as $d$ increases.

Finally, for the particular cases of image and Fourier transform conditions, transverse magnifications are given by $H_2(z_{\rm im})$ and $B(z_{\rm ft})$, respectively.[9] For conventional images there is no dependence of transverse magnification on curvature radius $d$ of the incident beam, in contrast to what happens for Talbot images.

## 5. TALBOT IMAGES: ANGULAR MAGNIFICATION

In conventional images all the rays coming from one point at the input pass through only one point at the output. The angular magnification is defined by the output/input relationship between angles for any ray. In Talbot images this definition is not applicable because rays coming from a point at the input pass through different points at the output. To study output/input angle transformation, it will be necessary to establish some criteria. We propose two criteria. The first one defines the angular magnification as the output/input relationship of the slope variation between two rays that, coming from different positions at the input ($z = 0$), intersect at the same point at $z_{\beta'/\alpha'}$ with consecutive slopes [Fig. 5(a)]. In the second criterion, angular magnification is stated as the output/input relationship of the slope variation between two rays of consecutive diffraction orders that, coming from the same position at the input, do not intersect at $z_{\beta'/\alpha'}$ [Fig. 5(b)].

To apply the first criterion, we determine conditions for which rays at the input coming from different positions intersect at the same point with consecutive slopes on a fractional Talbot plane. Such conditions can be found if slopes of rays at $z_{\beta'/\alpha'}$ are written as

$$\dot{x}(z_{\beta'/\alpha'}) = \dot{x}(z_{\beta'/\alpha'}; u) + t\Delta\dot{x}(z_{\beta'/\alpha'}), \tag{58}$$

where

$$\dot{x}(z_{\beta'/\alpha'}; u) = u[p\dot{A}(z_{\beta'/\alpha'})\bar{h} + \bar{m}\dot{B}(z_{\beta'/\alpha'})], \tag{59}$$

$$\Delta\dot{x}(z_{\beta'/\alpha'}) = p\dot{A}(z_{\beta'/\alpha'})[\alpha'\dot{\xi}(z_{\beta'/\alpha'} - \beta')], \tag{60}$$

and Eqs. (13), (14), and (35) have been used. Note that Eq. (59) depends on the intracell number and $z_{\beta'/\alpha'}$, whereas Eq. (60) depends only on the Talbot position. Thus the slope variation between two rays passing through the same point on $z_{\beta'/\alpha'}$ is given by

$$\dot{x}'(z_{\beta'/\alpha'}) - \dot{x}(z_{\beta'/\alpha'}) = (\tilde{t} - t)\Delta\dot{x}(z_{\beta'/\alpha'}) = \Delta t\Delta\dot{x}(z_{\beta'/\alpha'}), \tag{61}$$

and for two consecutive rays, in which $\Delta t = 1$ in Eq. (61), the equation becomes Eq. (60). In this case, taking into account Eqs. (35), it follows that the conditions for two rays intersecting at $z_{\beta'/\alpha'}$ are the following: The difference between cell numbers and diffraction orders must be $-\beta'$ and $\alpha'$, respectively [Fig. 5(a)]. Likewise, Eq. (60) at the input, $z = 0$, reduces to

$$\Delta\dot{x}_0 = \frac{\lambda d\alpha' - p^2\beta'}{n_0 pd}, \tag{62}$$

where Eqs. (14) and (15), evaluated at $z = 0$, and Eqs. (9b) and (10b) have been used.

From Eqs. (60) and (62) it follows that the angular magnification for the first criterion is given by

$$M_a^{(1)} = \frac{\Delta\dot{x}(z_{\beta'/\alpha'})}{\Delta\dot{x}_0} = \frac{n_0p^2d\dot{A}(z_{\beta'/\alpha'})[\alpha'\dot{\xi}(z_{\beta'/\alpha'}) - \beta']}{\lambda d\alpha' - p^2\beta'}$$
$$= \frac{n_0p^2d\dot{A}(z_{\beta'/\alpha'})[\dot{\xi}(z_{\beta'/\alpha'}) - \xi(z_{\beta'/\alpha'})]}{\lambda d - p^2\xi(z_{\beta'/\alpha'})}, \tag{63}$$

where Eq. (24) has been used.

Equation (63) can be rewritten as

$$M_a^{(1)} = H_2^{-1}(z_{\beta'/\alpha'}), \tag{64}$$

where Eqs. (11) and (14)–(16) have been used.

Equation (63) for integer Talbot images becomes

$$M_a^{(1)} = H_2^{-1}(z_\nu). \tag{65}$$

Thus angular magnification is given by the inverse value of the field ray position at Talbot images.

We now apply the second criterion to evaluate the angular magnification. First, we determine condition of position difference at $z_{\beta'/\alpha'}$ between rays coming from the same input point with consecutive diffraction orders. With this in mind, the requirement that

$$\Delta \tilde{m} = (u' - u)\bar{m} + \alpha'(\tilde{t} - t) = 1 \tag{66}$$

must hold, and then

$$\tilde{t} - t = \frac{1 - (u' - u)\bar{m}}{\alpha'}, \tag{67}$$

where Eq. (35b) has been used.

From Eqs. (13) and (35a), position difference is given by

$$\begin{aligned}\Delta x = x' - x &= pA(z_{\beta'/\alpha'})[\bar{h}' + (\bar{m} + 1)\xi(z_{\beta'/\alpha'}) - \bar{h} \\ &\quad - \bar{m}\xi(z_{\beta'/\alpha'})] \\ &= pA(z_{\beta'/\alpha'})[\bar{h}(u' - u) - \beta'(\tilde{t} - t) + \xi(z_{\beta'/\alpha'})].\end{aligned} \tag{68}$$

Substitution of Eq. (67) into Eq. (68) gives

$$\begin{aligned}\Delta x &= pA(z_{\beta'/\alpha'})\{[\bar{h} + \xi(z_{\beta'/\alpha'})\bar{m}](u' - u)\} \\ &= \frac{pA(z_{\beta'/\alpha'})(u' - u)}{\alpha'},\end{aligned} \tag{69}$$

where Eqs. (34) and (24) have been used.

From Eq. (69) it follows that position difference at $z_{\beta'/\alpha'}$ for rays coming from the same position with consecutive diffraction orders depends on the difference between the intracell numbers and on the intracell period.

For application of the second criterion, the slope variation between two rays with consecutive diffraction orders starting from the same position that do not intersect at $z_{\beta'/\alpha'}$ is given by

$$\begin{aligned}\Delta \dot{x}_{\beta'/\alpha'} &= p\dot{A}(z_{\beta'/\alpha'}\{\bar{h} + (\bar{m} + 1)\dot{\xi}(z_{\beta'/\alpha'}) \\ &\quad - [\bar{h} + \bar{m}\dot{\xi}(z_{\beta'/\alpha'})]\} \\ &= p\dot{A}(z_{\beta'/\alpha'})\dot{\xi}(z_{\beta'/\alpha'}) = \dot{B}(z_{\beta'/\alpha'}),\end{aligned} \tag{70}$$

where Eqs. (13), (14), and (16) have been used.

Equation (70) at $z = 0$, taking into account Eqs. (9b) and (16), reduces to

$$\Delta \dot{x}_0 = \frac{\lambda}{n_0 p}. \tag{71}$$

Equations (70) and (71) give the angular magnification, which can be expressed as

$$M_a^{(2)} = \frac{\Delta \dot{x}_{\beta'/\alpha'}}{\Delta \dot{x}_0} = \dot{H}_1(z_{\beta'/\alpha'}), \tag{72}$$

where Eq. (16) has been used.

For integer Talbot images, Eq. (72) becomes

$$M_a^{(2)} = \dot{H}_1(z_\nu). \tag{73}$$

Then the angular magnification is given by the value of the axial ray slope at the Talbot planes.

From Eqs. (64) and (72), it follows that

$$M_a^{(1)}M_a^{(2)} = \frac{\dot{H}_1(z_{\beta'/\alpha'})}{H_2(z_{\beta'/\alpha'})} = \frac{g(z_{\beta'/\alpha'})}{g_0}, \tag{74}$$

where Eq. (8) has been used.

For a selfoc medium, in which $g(z)$ is a constant, Eq. (74) reduces to

$$M_a^{(1)}M_a^{(2)} = 1; \tag{75}$$

that is, the two criteria are reciprocal.

Figure 6 depicts angular magnification versus self-image number for the two criteria. Angular magnifica-

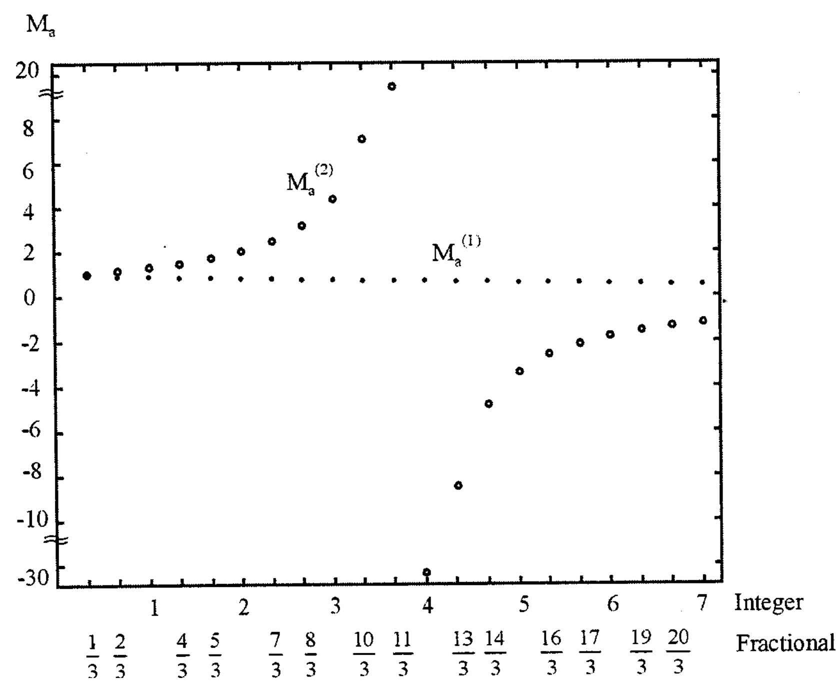


Fig. 6. Variation of the angular magnification with self-image number for the first and the second criteria. Calculations have been made for the values of Fig. 4 and $d = 15$ mm.

tion for first criterion, $M_a^{(1)}$, decreases slowly with the self-image number, and angular magnification $M_a^{(2)}$ for the second criterion changes, logically, the sign for the zeros of $H_2$, in which $M_a^{(2)}$ tends to infinity. The modulus of $M_a^{(2)}$ increases to the first zero of $H_2$ and decreases from this first zero.

Finally, note that number theory can be applied to the Talbot effect in free space (homogeneous medium), taking into account that $H_1(z) = z$, $H_2(z) = \dot{H}_1(z) = 1$, $\dot{H}_2(z) = 0$, and $n_0 = 1$.

## 6. TALBOT IMAGES FOR A FINITE NUMBER OF RAYS

The aim of this section is to evaluate the number of Talbot images that can be obtained for a finite number of rays and how these rays are distributed inside the unit cell at a fractional Talbot image. Let us consider now that for each point of the grating a finite number of $2M + 1$ diffracted rays is emitted.

The set of rays $R_u$ with cell numbers $\tilde{h}$ and slopes $\tilde{m}$ crossing through a point with intracell number $u$ at a plane $z_{\beta'/\alpha'}$ can be written as

$$R_u = \{(u\bar{h} - \beta' t, u\bar{m} + \alpha' t)/t \in Z\}, \qquad (76)$$

where Eqs. (35) have been used. For a finite number of rays with diffracted orders

$$-M, -M + 1, \ldots, 0,\ 1,\ 2, \ldots M - 1,\ M, \qquad (77)$$

we must force that the diffracted orders of rays crossing through $u$, Eq. (76), are contained in Eq. (77).

We know that the unit cell is formed by points $u = 0, 1, \ldots \alpha' - 1$ and that the orders of rays passing through each cell are different (see Section 4). Let us define the integer $r_u$, depending on the intracell number $u$, as the smaller diffracted order, positive integer or zero, crossing through the intracell number $u$:

$$0 \leqslant r_u < \alpha'. \qquad (78)$$

$r_u$ cannot be $r_u \geqslant \alpha'$, because if the difference between the diffracted orders passing through $u$ must be $\alpha'$, then for a given $u$ we can always have an $r_u$ lying in the range (78). With this definition we will denote the diffracted orders crossing through an intracell number by

$$m(u) = r_u \bmod \alpha' = r_u + \alpha' t, \qquad (79)$$

and consistently, since for a unit cell $r_u$ is in the range $r_u = 0, 1, \ldots, \alpha' - 1$, for any diffracted order $m$, $r_u$ is the residue of $m$ modulus $\alpha'$:

$$\mathrm{res}_{\mathrm{mod}\ \alpha'}(m) = r_u. \qquad (80)$$

This allows us to determine the position $u$ through which the diffracted order passes inside the unit cell. This result shows how to characterize rays crossing the unit cell. Note that for the integer Talbot image, in which there is only one point, all rays intersect at the same point in the unit cell.

The following step characterizes the fractional Talbot images ($\alpha' \geqslant 2$) that can be obtained for $2M + 1$ rays. For that, we have to distribute $2M + 1$ rays among the $\alpha'$ intracell points that constitute the unit cell. For visualization of a Talbot image, there will have to exist at least one intersection between two rays at one point on this plane.

Notice that the number of rays passing through different intracell points differs at most by one ray. Indeed, from the discussion leading to Eq. (80), it follows that the rays with orders $-M$, $-M + 1, \ldots, -M + \alpha' - 1$, cross through different intracell points characterized by $r_u$, $r_u = 0, 1, \ldots, \alpha' - 1$. The ray with diffracted order $-M + \alpha'$ will cross through the position of ray $-M$ and so on; then it is proved that the set of rays passing through different intracell points differs by zero or one. We will distribute the $2M + 1$ rays among the $\alpha'$ intracell points as follows:

$$2M + 1 = \alpha' C + R, \qquad 0 \leqslant R < \alpha', \qquad (81)$$

where $C$ is the greatest common number of rays passing through each intracell point and $R$ is the number of points of the unit cell through which one more ray passes.

In order to know how many Talbot images we can see, we are going to analyze which will be the last fractional image that is formed with $2M + 1$ rays. Then we will evaluate the first value of $\alpha'$ corresponding to the plane where there is no intersection between rays. In this case, from Eq. (81) it follows that $C = 1$ and $R = 0$ and thus $\alpha' = 2M + 1$. Similarly, the value of $\alpha'$ for which there is at least one intersection between two rays holds for $C = 1$, $R = 1$, and $\alpha' = 2M$. In short, for $2M + 1$ rays, we obtain between two consecutive integer Talbot images a set of fractional Talbot images $z_{\beta'/\alpha'}$ such that $\alpha' \leqslant 2M$.

The set of fractional Talbot images can be represented by the Farey series[10] $F_{2M}$ of order $2M$. It is the ascending series of irreducible fractions between 0 and 1 whose denominators do not exceed $2M$. This series includes the number 0 and 1 in the forms 0/1 and 1/1. In our case, the number of Talbot images will be given by the Farey series minus 1, since 0/1 represents the object at the input.

The number of Talbot images will be given by the Euler function $\phi(\alpha')$ (Ref. 10), which indicates the number of positive integers (zero is excluded) not greater than and prime to $\alpha'$, that is, the number of integers $\beta'$ such that

$$0 < \beta' \leqslant \alpha', \qquad \gcd(\alpha', \beta') = 1, \qquad (82)$$

where gcd is the greatest common divisor.

Since $\alpha' \in [2, 2M]$, the number of Talbot images that can be obtained for $2M + 1$ rays is given by

$$P_M = \sum_{\alpha'=2}^{2M} \phi(\alpha'), \qquad (83)$$

with

$$\phi(\alpha') = \alpha' \prod_{\beta'/\alpha'} (1 - 1/\beta'), \qquad (84)$$

where the product runs through a complete set of prime values $\beta'$ divisors of $\alpha'$.

We particularize this study to a GRIN medium with a divergent linear taper given by Eq. (57). Figure 7 depicts a set of fractional Talbot images obtained with five rays

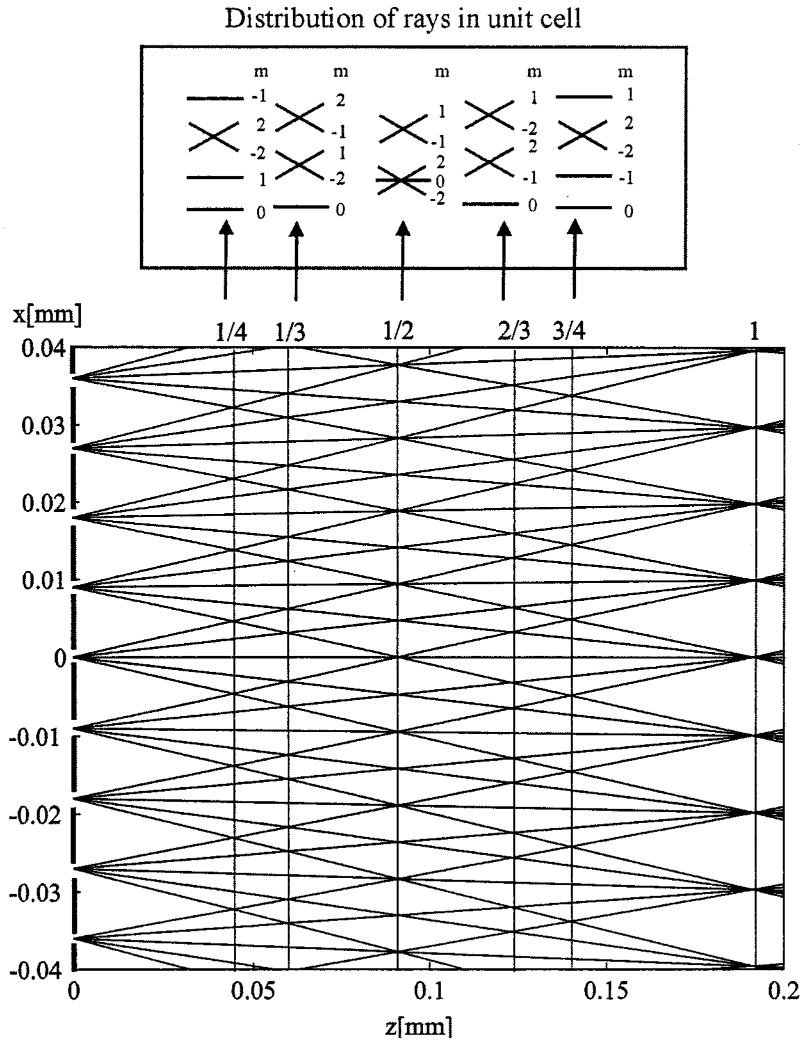


Fig. 7. Fractional and integer Talbot images in a GRIN medium obtained for five rays. Calculations have been made for the values of Fig. 4.

($M = 2$). At the top of the figure we represent the rays distribution inside unit cells for each fractional Talbot image. For simplicity, we present only the fractional Talbot images between the input and the first integer Talbot image ($\nu = 1$).

For $\alpha' = 2$ ($z_{1/2}$), the unit cell will be formed by two points, and from Eq. (81), that is, $C = 2$ and $R = 1$, we have one point obtained by the intersection of three rays and another point obtained by the intersection of two rays; in the case of $\alpha' = 3$ ($z_{1/3}, z_{2/3}$), the unit cell has three points with $C = 1$ and $R = 2$; in the case of $\alpha' = 4$ ($z_{1/4}, z_{3/4}$), the unit cell is formed by four points, with $C = 1$ and $R = 1$. Similarly, at the integer Talbot image, the five rays cross through the same point. Finally, the number of fractional Talbot images obtained for five rays is obtained from Eqs. (83) and (84); that is,

$$P_2 = \phi(2) + \phi(3) + \phi(4) = 5. \tag{85}$$

Note that the ray trajectories are quasi-linear owing to weak inhomogenety of the GRIN medium and the position of Talbot images close to the input.

## 7. CONCLUSIONS

A new interpretation of the Talbot effect by number theory as the output/input relationship between the integer and the noninteger difference of position and the slope of rays has been shown. In this framework, unit cell and transverse magnification for Talbot images has been evaluated, and two criteria for the angular magnification have been defined. We have the study particularized to a finite set of diffracted rays in order to find the number of fractional Talbot images that we can observe. Results have been applied to a particular case of a tapered GRIN medium.

## APPENDIX A

We wish to prove that the general solution of Eq. (32) for the cell number and diffraction order are given by Eqs. (35).

To find the general solution, first we assume a particular case of Eq. (32) such that

$$h\alpha' + m\beta' = 0; \tag{A1}$$

that is,

$$h/m = -\beta'/\alpha', \tag{A2}$$

where $\alpha'$, $\beta'$ are co-prime integers and $(h, m)$ must be integers; then the general solution can be written as

$$h = -\beta' t, \tag{A3}$$

$$m = \alpha' t, \tag{A4}$$

where $t$ is an integer number.

We now consider another particular case of Eq. (32):

$$h\alpha' + m\beta' = 1; \tag{A5}$$

this equation is solvable.[9,10] If we denote a particular solution of Eq. (A5) by $(\bar{h}, \bar{m})$, we can assume that the general solution of Eq. (A5) is given by

$$\tilde{h} = \bar{h} - \beta' t, \tag{A6}$$

$$\tilde{m} = \bar{m} + \alpha' t. \tag{A7}$$

In fact, if we express the general solution as $(\tilde{h}, \tilde{m})$ and the particular solution given by the Bézout theorem as $(\bar{h}, \bar{m})$, the following equations,

$$\text{hypothesis:} \quad \alpha'\tilde{h} + \beta'\tilde{m} = 1, \tag{A8}$$

$$\text{Bézout solution:} \quad \alpha'\bar{h} + \beta'\bar{m} = 1, \tag{A9}$$

must be satisfied, and then

$$\alpha'(\tilde{h} - \bar{h}) + \beta'(\tilde{m} - \bar{m}) = 0. \tag{A10}$$

So, from Eqs. (A6) and (A7), the differences $(\tilde{h} - \bar{h}, \tilde{m} - \bar{m})$ satisfy Eq. (A10), and it is proved that Eqs. (A6) and (A7) are solutions of Eq. (A5).

Finally, to find the solution of Eq. (32), it is enough to observe that the particular solution $(\bar{h}, \bar{m})$ becomes $(u\bar{h}, u\bar{m})$, so the general solution is achieved from Eqs. (A6) and (A7) by replacing the particular solution $(\bar{h}, \bar{m})$ with $(u\bar{h}, u\bar{m})$. Thus the general solution is given by Eqs. (35).

## ACKNOWLEDGMENT

This work was supported by the Ministerio de Educación y Cultura, Spain, under contract TIC99-0489.

Corresponding author Carlos Gómez-Reino can be reached by phone/fax, 349-815-21984 or by e-mail, facgrc@usc.es.

## REFERENCES

1. K. Patorski, "The self-imaging phenomenon and its applications," in *Progress in Optics XXVII*, E. Wolf, ed. (North-Holland, Amsterdam, 1989), pp. 3–101 and references therein.
2. M. V. Berry and S. Klein, "Integer, fractional and fractal Talbot effects," J. Mod. Opt. **43**, 2139–2164 (1996) and references therein.
3. M. T. Flores-Arias, C. Bao, M. V. Pérez, and C. Gómez-Reino, "Talbot effect in a tapered gradient-index medium for nonuniform and uniform illumination," J. Opt. Soc. Am. A **16**, 2439–2446 (1999).
4. M. T. Flores-Arias, C. R. Fernández-Pousa, M. V. Pérez, C. Bao, and C. Gómez-Reino, "Fractional Talbot effect in a tapered gradient-index medium: unit cell," J. Opt. Soc. Am. A **17**, 1007–1011 (2000).
5. P. Latimer and R. F. Course, "Talbot effect reinterpreted," Appl. Opt. **31**, 80–89 (1992).
6. P. Szwaykowski, "Talbot effect reinterpreted: comment," Appl. Opt. **32**, 3466–3467 (1993).
7. P. Latimer, "Talbot effect reinterpreted: reply to comment," Appl. Opt. **32**, 3468–3469 (1993).
8. P. Szwaykowski and J. Ojeda-Castañeda, "Nondiffracting beams and the self-imaging phenomenon," Opt. Commun. **83**, 1–4 (1991).
9. C. Gómez-Reino, "GRIN optics and its applications in optical connections," Int. J. Optoelectron. **7**, 607–680 (1992).
10. G. H. Gardy and E. M. Wright, *An Introduction to the Theory of Number*, 5th ed. (Clarendon, Oxford, UK, 1995), pp. 21, 23, 52, 53.
11. J. C. Fernando and V. Gregori, *Matemática Discreta* (Editorial Reverté, Barcelona, Spain, 1994), p. 98.